

## Spin Squeezed Atoms: A Macroscopic Entangled Ensemble Created by Light

J. Hald, J. L. Sørensen, C. Schori, and E. S. Polzik

*Institute of Physics and Astronomy, Aarhus University, Aarhus, 8000 Denmark*

(Received 21 January 1999)

We report on the experimental observation of a spin squeezed ensemble of  $10^7$  cold atoms. This macroscopic ensemble is generated via quantum state transfer from nonclassical light to atoms.

PACS numbers: 42.50.Ct, 03.65.Bz, 42.50.Dv, 42.50.Lc

Quantum correlated systems of atoms and ions have recently attracted considerable attention. Prime motivations for that come from the fields of quantum information and measurements beyond quantum limits. In the first of these two areas, quantum correlations or entanglement between particles open up new possibilities for data processing [1]. An important and unresolved issue in this domain is how to map quantum states of light (the prime carrier) onto quantum states of atoms (possible storage medium). In the second area, the sensitivity at the “standard quantum limit” (SQL) set by the quantum noise of individual uncorrelated particles has been demonstrated in several experiments with atoms and ions. In particular, quantum limits have been reached for a cesium fountain frequency standard [2], for a collection of cold ions in a trap [3], and for polarization interferometry of cold atoms [4]. Entanglement between individual particles opens up a possibility to overcome these limits.

The atom-atom entanglement can be produced by a nonlinear spin-spin interaction as proposed in [5] and recently demonstrated for two ions in a trap [6]. The entanglement of two atoms via interaction with optical cavity fields has been investigated theoretically in [7]. In Ref. [8] the two-atom entanglement via interaction with a microwave cavity field has been experimentally demonstrated. Production of quantum correlated atomic states via quantum nondemolition (QND) measurements has been considered in [9].

In this Letter we report on the generation of a macroscopic entangled atomic ensemble. The results present an experimental realization of a recent proposal [10,11] of a method for the generation of quantum correlated atomic ensembles. The proposal involves mapping of a state of free propagating quantum correlated light onto an atomic ensemble, and therefore is relevant for the problem of storage of the entanglement of light in atoms. More precisely, we produce spin squeezed atomic states via mapping of the squeezed light onto atoms as proposed in [10]. Because of the *multiparticle nature* of the produced entanglement, the proposal has also been attractive for the atomic ensemble spin polarization measurements [2–4].

Consider an atomic ensemble in an excited state. The spin polarization of this state (in this Letter it is the  $6P_{3/2}$ ,  $F = 5$  state of cesium, hereby abbreviated as  $6P$ , Fig. 1) is described by a collective spin operator  $\hat{J}$ . If the state

is excited with light linearly polarized along the  $x$  axis, it becomes aligned along the  $x$  axis with  $\langle \hat{J}_x^2 - \hat{J}_y^2 \rangle \neq 0$ . Then the commutation relation  $\frac{i}{2}[\hat{J}_z, \hat{J}_x\hat{J}_y + \hat{J}_y\hat{J}_x] = \hat{J}_x^2 - \hat{J}_y^2$  leads to the quantum uncertainty for the spin projection  $\hat{J}_z$  along the direction of light propagation (Fig. 1),  $\delta(\hat{J}_z)\delta(\hat{J}_x\hat{J}_y + \hat{J}_y\hat{J}_x) \geq |\langle \hat{J}_x^2 - \hat{J}_y^2 \rangle|$ . In the case of uncorrelated individual atomic spins corresponding to excitation with coherent light, this uncertainty takes the value  $\delta(\hat{J}_z)_{\text{coh}} \propto \sqrt{N}$ , where  $N$  is the number of atoms in  $6P$  state. This value sets the quantum limit on the smallest detectable projection  $\hat{J}_z$  of the aligned atomic state. As demonstrated in this Letter, entanglement of individual atoms produced by excitation with quantum correlated, squeezed light leads to the uncertainty beyond the quantum limit  $\delta(\hat{J}_z)_{\text{sq}} < \delta(\hat{J}_z)_{\text{coh}}$ . This inequality defines our spin squeezed ensemble.

The adopted definition of the spin squeezing is one of the possible multilevel generalizations of the two-level definition introduced in [5]. Indeed, two-level atoms considered in [3,5] are completely described by the orientation vector  $\hat{J}_{x,y,z}$  obeying  $[\hat{J}_x, \hat{J}_y] = i\hat{J}_z$  with the corresponding uncertainty relation. Spin squeezing can then be defined via the quantum limit of uncertainty for uncorrelated atoms as  $\delta(\hat{J}_z)'_{\text{sq}} < \delta(\hat{J}_z)'_{\text{coh}} = \sqrt{\langle \hat{J}_y \rangle} / 2$  for

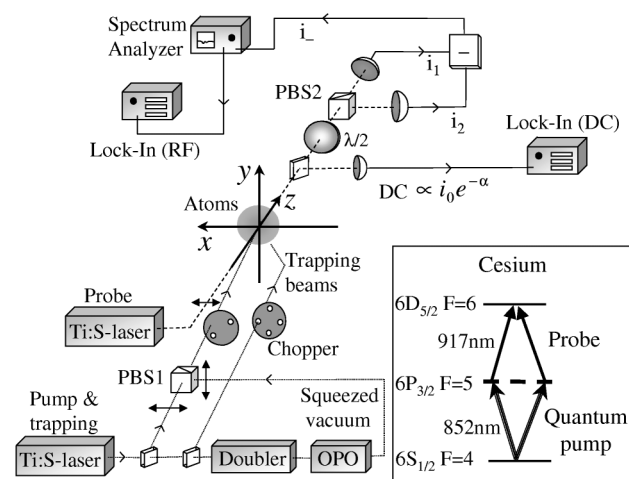


FIG. 1. Generation of the spin squeezed atomic ensemble via entanglement exchange with the quantum pump. The inset shows the level scheme with spin squeezing generated in the  $6P$  state.

an ensemble oriented along the  $y$  axis. For atoms with more than two levels, e.g., in a magnetically degenerate  $6P$  state, the spin polarization, in general, is described by higher order polarization moments. Accordingly, other uncertainty relations can be used to define and analyze a spin polarization squeezed state. A common feature for all of these types of spin squeezing is the reduction of quantum fluctuations of some spin polarization component beyond the level set for uncorrelated atoms by the corresponding commutation relation.

Turning now to the experiment, we collect about  $10^9$  Cs atoms in a magneto-optical trap and study the spin of the  $6P$  state using the probe polarization noise technique developed in Ref. [4] (Fig. 1). According to [4] the change in the probe differential photocurrent noise caused by atoms is

$$\delta i^2(\Delta) = -[1 - \exp(-\alpha_\Delta)] + s\alpha_0 \exp(-2\alpha_\Delta) (\delta\tilde{J})^2,$$

where  $(\delta\tilde{J})^2$  is the atomic noise contribution per atom depending on the geometry of the experiment,  $\alpha_\Delta$  is the probe optical depth at detuning  $\Delta$ , and  $s$  is the probe saturation parameter. The expression for  $\delta i^2$  is normalized to the probe shot noise in the absence of atoms. The term in square brackets is the probe shot noise reduction  $\delta i_{\text{shot}}^2$  due to the absorption, and the rest is the atomic noise contribution of interest. In our experiment the shot noise reduction dominates over the atomic noise leading to a negative  $\delta i^2$ . To observe  $\delta i^2$  the trapping beams and the magnetic field are chopped at 450 Hz and the spin state of the  $6P$  ensemble is studied only during the 1.2 ms “dark” period by the lock-in technique. During every second dark period the quantum pump is turned on. In this way the  $6P$  state is modulated at 225 Hz providing the possibility for lock-in discrimination of the noise against the background of the major part of the probe shot noise and the electronic dark noise. The measured lock-in voltage is then proportional to  $\delta i^2(\Delta)$ .

For the probe geometry of Fig. 1 [4,12],

$$(\delta\tilde{J})^2 = \kappa_L L^2(\Delta) [\delta(\hat{J}_x \hat{J}_y + \hat{J}_y \hat{J}_x)]^2 + \kappa_D D^2(\Delta) (\delta\hat{J}_z)^2,$$

$L(\Delta) + iD(\Delta) = \gamma/(\gamma + i\Delta)$ ,  $\gamma$  is the linewidth of the probe transition, and  $\kappa_L, \kappa_D$  depend on atomic parameters. Depending on the detuning  $\Delta$  and  $\kappa_L, \kappa_D$  the noise of one of the two conjugated variables  $\hat{J}_z$  and  $\hat{J}_x \hat{J}_y + \hat{J}_y \hat{J}_x$  may be analyzed.

First we excite the  $6P$  collective spin with the coherent pump polarized along  $x$  in order to establish the quantum limit of the spin noise. The  $50 \mu\text{W}$  pump with a beam diameter of 4.0 mm resonant with the  $6S_{1/2}, F = 4 \rightarrow 6P_{3/2}, F = 5$ , 852 nm transition provides weak excitation for the  $6P$  collective spin of about  $10^7$  atoms. The probe is linearly polarized parallel to the coherent component of the pump and near resonant with the  $6P_{3/2}, F = 5 \rightarrow 6D_{5/2}, F = 6$ , 917 nm transition. The probe beam diameter is 3.7 mm and the power is about  $250 \mu\text{W}$  for the off-resonant spin squeezing measurements ( $s = 0.4$ ).

The polarization noise of the probe is analyzed by the balanced polarization interferometer and the spectrum analyzer (SA) set at  $\Omega/2\pi = 1.9$  MHz with the resolution bandwidth 300 kHz, video bandwidth 10 kHz, and zero frequency span [4]. The output of the SA is fed into the lock-in amplifier synchronized with the 225 Hz frequency of the chopper. We measure  $\delta i^2(\Delta) = -\delta i_{\text{shot}}^2(\Delta) + \delta i_{\text{coh}}^2(\Delta)$  with  $\delta i_{\text{coh}}^2$  as the quantum spin noise. The value of  $\delta i_{\text{shot}}^2(\Delta)$  is measured independently via sending the probe through a passive absorber modulated at 225 Hz. We plot in Fig. 2  $[1 + \delta i^2(0)] \exp(\alpha_0)$  as a function of  $\alpha_0$  for the passive absorber (triangles,  $\delta i^2 = -\delta i_{\text{shot}}^2$ ) and for the coherently excited atoms (dots). The fit confirms that  $\delta i_{\text{coh}}^2(0) \propto \alpha_0 \propto N$  for small  $\alpha_0$ , and therefore we indeed measure the quantum spin noise of independent atoms.  $\alpha_\Delta$  is measured by splitting 4% of the probe onto a dc detector followed by a lock-in amplifier measuring the modulation depth  $1 - \exp(-\alpha_\Delta)$  (Fig. 1). Now fixing  $\alpha_0$  at its maximal value, we measure the spectral distribution of the coherent spin noise by scanning the probe detuning (Fig. 3, dots). The spectrum of the spin noise,  $\delta i_{\text{coh}}^2(\Delta)$ , contains a resonant absorptive contribution as well as an off-resonant dispersive contribution from fluctuations in  $\hat{J}_z$ . The suitably normalized square of the dc absorption spectrum is shown in Fig. 3 (triangles). The atomic sample is accelerated and heated by the pump during the 1.2 ms measurement time. This results in Doppler broadening comparable to the natural linewidth included by fitting the absorption spectrum to a Voigt profile. It is clear from Fig. 3 that the off-resonant noise caused by  $\hat{J}_z$  fluctuations dominates in the wings of the coherent spin noise spectrum.

We proceed by injecting frequency tunable squeezed vacuum [13,14] polarized along the  $y$  axis into the second port of PBS1 in addition to the coherent pump polarized along  $x$ . The squeezed light after PBS1 will have fluctuations in either the polarization axis direction or in the

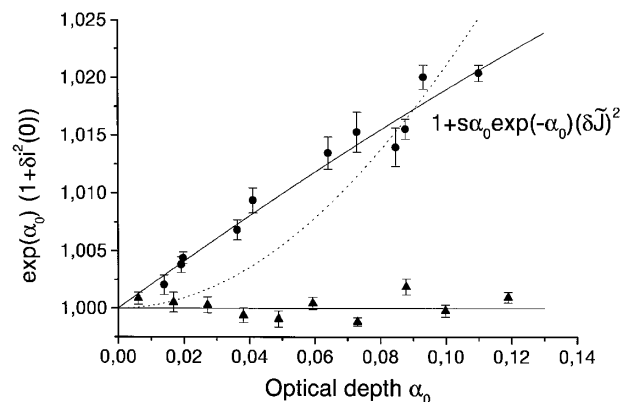


FIG. 2. Probe noise for coherent spin excitation and  $s = 1$ ,  $\Delta = 0$ . Triangles: probe shot noise. Dots: additional probe noise due to atomic spin noise. Solid line: fit to quantum spin noise model  $1 + s\alpha_0 \exp(-\alpha_0) (\delta\tilde{J})^2$ . Dotted curve: best fit to the classical spin noise model  $1 + s\alpha_0^2 \exp(-\alpha_0) (\delta\tilde{J})^2$ .

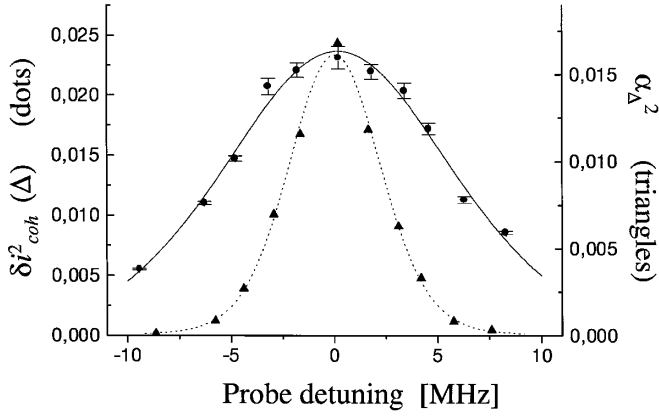


FIG. 3. Triangles (right axis): probe optical depth squared  $\alpha_{\Delta}^2$ . Dots (left axis): coherent spin noise  $\delta i_{\text{coh}}^2(\Delta)$ . Solid line: smooth curve through data points. Dotted line: squared Doppler broadened Lorentzian.

ellipticity (depending on the phase) reduced below the noise level of the coherent field (SQL) [14]. For the ellipticity-squeezed light, the fluctuations in the intensity difference between the  $\sigma^+$ - and  $\sigma^-$ -polarized components of the pump field are reduced below the SQL. This gives reduced fluctuations in the difference between the number of atoms in the  $+m$  and  $-m$  Zeeman levels. This difference in populations is described quantitatively by the collective spin component  $\hat{J}_z$ . Thus, the ellipticity-squeezed light gives reduced fluctuations in  $\hat{J}_z$ , whereas the polarization-squeezed light is antisqueezed in ellipticity resulting in increased  $\hat{J}_z$  noise and reduced  $\hat{J}_x\hat{J}_y + \hat{J}_y\hat{J}_x$  noise. The amount of squeezing of light is quantified by the variance of the quadrature phase operator  $X_{\pi/2}^2$  of the electromagnetic field polarized along  $y$  and out of phase with the coherent component of the pump. For perfectly squeezed ellipticity  $X_{\pi/2}^2 = 0$  and for coherent fields and/or ordinary vacuum  $4X_{\pi/2}^2 = 1$ . In order to achieve the best mapping of quantum properties of light onto atoms [10], the optical depth for the quantum pump is sustained at the highest possible level,  $\alpha_{\text{pump}} \approx 4$ . We concentrate on the measurement of  $\delta J_z$  because the sensitivity of our polarization measurements to squeezing of the conjugated variable  $\delta(\hat{J}_x\hat{J}_y + \hat{J}_y\hat{J}_x)$ , the alignment in the  $\pm 45^\circ$  coordinate system, is found to be much smaller, the fact predicted theoretically and confirmed experimentally.

Operationally the phase of the squeezed vacuum is stabilized by standard methods [14] during the trapping periods when the quantum pump is reflected off the gold-plated surface of the chopper onto a pair of balanced detectors [15]. When the squeezed vacuum is out of phase with the coherent component of the pump,  $4X_{\pi/2}^2 > 1$ . This phase corresponds to the quantum noise of the spin component  $\hat{J}_z$  above the coherent spin noise level. The observed excess noise is plotted in Fig. 4 as dots. The spectrum of the observed antisqueezed excess spin noise can be written as  $\delta i_{\text{antisq}}^2(\Delta) - \delta i_{\text{coh}}^2(\Delta) \propto$

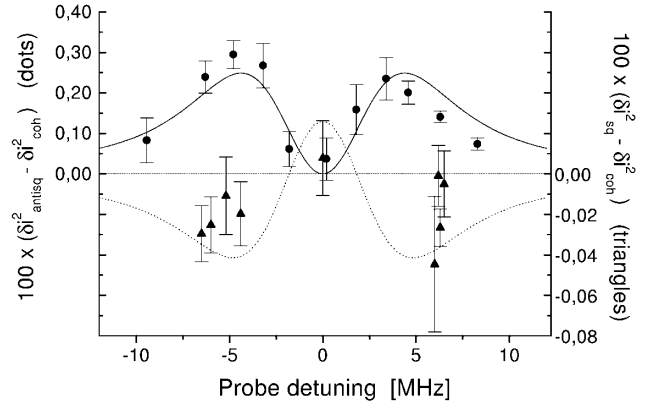


FIG. 4. Squeezed spin noise of atoms. Dashed line at zero: spin noise for uncorrelated atoms. Dots (left axis): antisqueezed spin noise. Triangles (right axis): squeezed spin noise. Solid line: square Doppler broadened dispersion function. Dotted line: expected spin squeezing spectrum. The detuning uncertainty is 0.5 MHz. Note that the scales for spin squeezing and spin antisqueezing are different.

$\bar{D}^2(\Delta)[(\delta \hat{J}_z)^2 - (\delta \hat{J}_z)_{\text{coh}}^2]$ , where the contribution from squeezed  $\hat{J}_x\hat{J}_y + \hat{J}_y\hat{J}_x$  has been neglected. The excess spin noise is expected to have the spectral shape given by the square of the Doppler broadened dispersion profile  $\bar{D}^2(\Delta)$ . This profile with the linewidths taken from the dc absorption spectrum (Fig. 3) and only the amplitude as a free parameter is plotted as a solid line in Fig. 4. We introduce  $\eta$ , the mapping-readout efficiency for quantum correlations, by relating the observed spin noise to  $4X_{\pi/2}^2$ . With  $\Delta_{\text{max}}$  being the detuning giving the maximum excess noise we get  $\delta i_{\text{antisq}}^2(\Delta_{\text{max}}) = \frac{1}{\eta+1}(1 + \eta 4X_{\pi/2}^2)\delta i_{\text{coh}}^2(\Delta_{\text{max}})$ .  $\eta = 1$  gives 50% noise reduction for perfect squeezing and is the theoretical maximum efficiency in a three-level system when the spontaneous decay is taken into account [10]. For a multilevel system the exact role of the spontaneous decay is unknown and it might set an upper limit on  $\eta$  below 1 in this experiment. The data in Fig. 4 corresponds to  $(4.5 \pm 0.6)$  dB of the excess noise in the antisqueezed quadrature of the pump giving  $4X_{\pi/2}^2 \approx 2.8$ . We obtain the value of the mapping-readout efficiency  $\eta = 0.09 \pm 0.02$ . The imperfect efficiency can be caused by many factors, including the multilevel effects, imperfect polarizations, the residual magnetic field, imperfect overlap of the pump and the probe, reabsorption of uncorrelated spontaneously emitted photons at 852 nm, and the finite bandwidth of the squeezed light. With the squeezed vacuum in phase, we measure  $\delta i_{\text{sq}}^2(\Delta_{\text{max}})$ . The average squeezing of the pump light available at the trap site is  $(-1.8 \pm 0.2)$  dB corresponding to  $4X_{\pi/2}^2 \approx 0.65$ . The expected quantum spin noise spectrum for such a pump and the efficiency  $\eta = 0.09$  is plotted as a dotted line in Fig. 4. Note that the resonant contribution from the antisqueezed  $\hat{J}_x\hat{J}_y + \hat{J}_y\hat{J}_x$  component leads to the antisqueezed spin noise

around zero detuning. Note also that the mapping-readout efficiency for the alignment component,  $\eta_{\text{alignment}} \approx 6 \times 10^{-3}$  is much less than  $\eta$ , as discussed above. The experimental data is plotted as triangles. All available experimental data obtained in nine runs, each lasting between 4 and 11 hours, are shown. The long integration time is needed even with all of the implemented lock-in detection stages because the quantum spin noise reduction corresponds to only  $\approx 2 \times 10^{-4}$  of the probe shot noise. Each point in the figure is the average of one run with 13 to 45 individual measurements. Each of these individual measurements consists of 6 min of averaging with the squeezed vacuum interacting with the atoms, and 6 min of averaging with the squeezed vacuum blocked.

We define the degree of the *observed* spin squeezing (quantum spin noise reduction) by  $\xi = (\delta i_{\text{sq}}^2 - \delta i_{\text{coh}}^2) / \delta i_{\text{coh}}^2$ . The best experimental points in Fig. 4 are in reasonable agreement with the expected degree of the quantum spin noise reduction which is  $-3.0\%$  at  $\pm 6$  MHz. The average value for all of the 183 individual measurements at  $\pm 6$  MHz is  $\xi = -(1.4 \pm 0.4)\%$ . Since we do not know what the relative contribution of the readout efficiency is out of the overall efficiency  $\eta$ , we cannot infer the actual degree of spin squeezing of atoms, but we can be sure that it is greater than the observed spin noise reduction  $\xi$ .

The macroscopic spin squeezed ensemble described above possesses quantum correlations or entanglement between individual atoms. Consider for simplicity an ensemble of  $N$  uncorrelated spins  $\frac{1}{2}$  with all of the atoms in the  $|+\frac{1}{2}\rangle$  state along the  $x$  axis (coherent spin state). The projection of the collective spin state on the  $z$  axis can then be written as  $\Psi'_{\text{uncorr}} \propto (|\frac{1}{2}\rangle + |-\frac{1}{2}\rangle)^N$ . The variance of this distribution is  $(\delta \hat{J}_z^2)_{\text{coh}}' = N/4$ . A state with the *same mean spin projections* (for large  $N$ ) and  $(\delta \hat{J}_z^2)' < (\delta \hat{J}_z^2)_{\text{coh}}'$  is not a product state of individual atoms, i.e., is an entangled state. The spin polarized ensemble described in this Letter also obeys  $\delta J_z^2 < (\delta J_z^2)_{\text{coh}}$  [although with a different value of  $(\delta J_z^2)_{\text{coh}}$ ] and therefore is also an entangled ensemble. We note that under the conditions of our experiment the mean spin of the ensemble indeed stays unchanged to a great accuracy during measurements of  $(\delta J_z^2)_{\text{sq}}$  and  $(\delta J_z^2)_{\text{coh}}$ , i.e., with and without squeezed vacuum injection. Injection of the squeezed vacuum cannot cause an alteration of the mean spin polarization by much more than the ratio of the squeezed vacuum power to the coherent pump power which is of the order of  $10^{-8}$ . Therefore we can safely rule out a possibility that the observed quantum noise reduction is caused by a trivial rotation of the mean spin polarization.

In summary, we have demonstrated experimentally the squeezed spin state for a macroscopic atomic ensemble.

The level of the collective spin noise below the quantum limit corresponding to uncorrelated atoms has been observed. The nonclassical atomic state is generated via entanglement exchange with the quantum correlated light completely absorbed in the process. The resulting atomic ensemble is an example of a macroscopic entangled object.

The results reported in this Letter prove the possibility of mapping a quantum state of free propagating light onto a multiatom ensemble, but the described method is not limited to squeezed states. Exciting candidates in the future may be, e.g., single photon states. An attractive avenue for future studies is to study mapping onto long lived atomic states. Besides the obvious advantages for “quantum memory” and sensitive measurements, such states are expected to yield a much better sensitivity to the spin noise [4] as well as to allow application of efficient atom counting techniques [2] for the atomic state analysis.

This research has been supported by the Danish Research Council and by the Thomas B. Thriges Center for Quantum Information.

- 
- [1] Special issue on Quantum Information, Phys. World (1998).
  - [2] G. Santarelli, Ph. Laurent, P. Lemonde, A. Clairon, A. G. Mann, S. Chang, A. N. Luiten, and C. Salomon, Phys. Rev. Lett. **82**, 4619 (1999).
  - [3] W. M. Itano, J. C. Bergquist, J. J. Bollinger, J. M. Gilligan, D. J. Heinzen, F. L. Moore, M. G. Raizen, and D. J. Wineland, Phys. Rev. A **47**, 3554 (1993).
  - [4] J. L. Sørensen, J. Hald, and E. S. Polzik, Phys. Rev. Lett. **80**, 3487 (1998).
  - [5] M. Kitagawa and M. Ueda, Phys. Rev. A **47**, 5138 (1993); D. J. Wineland, J. J. Bollinger, W. M. Itano, F. L. Moore, and D. J. Heinzen, Phys. Rev. A **46**, R6797 (1992).
  - [6] Q. A. Turchette, C. S. Wood, B. E. King, C. J. Myatt, D. Leibfried, W. M. Itano, C. Monroe, and D. J. Wineland, Phys. Rev. Lett. **81**, 3631 (1998).
  - [7] R. Walser, J. I. Cirac, and P. Zoller, Phys. Rev. Lett. **77**, 2658 (1996).
  - [8] E. Hagley, X. Maitre, G. Nogues, C. Wunderlich, M. Brune, J. M. Raimond, and S. Haroche, Phys. Rev. Lett. **79**, 1 (1997).
  - [9] A. Kuzmich, N. P. Bigelow, and L. Mandel, Europhys. Lett. **42**, 481 (1998).
  - [10] A. Kuzmich, K. Mølmer, and E. S. Polzik, Phys. Rev. Lett. **79**, 4782 (1997).
  - [11] E. S. Polzik, Phys. Rev. A **59**, 4202 (1999).
  - [12] F. Laloë, M. Leduc, and P. Miguzzi, J. Phys. **30**, 277 (1969).
  - [13] E. S. Polzik, J. Carri, and H. J. Kimble, Phys. Rev. Lett. **68**, 3020 (1992); Appl. Phys. B **55**, 279 (1992).
  - [14] E. S. Polzik, J. L. Sørensen, and J. Hald, Appl. Phys. B **66**, 759 (1998).
  - [15] We wish to thank Dr. J. Chevallier for the skillful coating of the chopper.